Detection of Microwave Spin Pumping Using the Inverse Spin Hall Effect

C Hahn, G De Loubens, M Viret, Olivier Klein, V.V. Naletov, J Youssef

Detection of the microwave spin pumping using the inverse spin Hall effect

C. Hahn, G. de Loubens, M. Viret, and O. Klein*

Service de Physique de l'État Condensé (CNRS URA 2464),

CEA Saclay, 91191 Gif-sur-Yvette, France

V.V. Naletov

Service de Physique de l'État Condensé (CNRS URA 2464),

CEA Saclay, 91191 Gif-sur-Yvette, France

Institute of Physics, Kazan Federal University, Kazan 420008, Russian Federation

J. Ben Youssef

Université de Bretagne Occidentale,

Laboratoire de Magnétisme de Bretagne CNRS,

6 Avenue Le Gorgeu, 29285 Brest, France

Abstract

We report on the electrical detection of the dynamical part of the spin pumping current emitted during ferromagnetic resonance (FMR) using the inverse Spin Hall Effect (ISHE). The experiment is performed on a YIG|Pt bilayer. The choice of YIG, a magnetic insulator, ensures that no charge current flows between the two layers and only the pure spin current produced by the magnetization dynamics is transferred into the adjacent strong spin-orbit Pt layer via spin pumping. To avoid measuring the parasitic eddy currents induced at the frequency of the microwave source, a resonance at half the frequency is induced using parametric excitation in the parallel geometry. Triggering this nonlinear effect allows to directly detect on a spectrum analyzer the microwave component of the ISHE voltage. Signals as large as 30 μV are measured for precession angles of a couple of degrees. This direct detection provides a novel efficient means to study magnetization dynamics on a very wide frequency range with great sensitivity.

One great expectation of spintronics regarding information technology is the promise that pure spin currents can be generated and manipulated without their charge current counterparts [1]. Pure spin currents correspond to the transport of angular momentum in a very wide range of materials including metals and insulators with or without magnetic order. In ferromagnetic metals, charge currents are intrinsically associated to spin currents because electrons at the Fermi level are spin polarized. Using these as injection electrodes, pure spin currents can be generated into a non magnetic metal in a non-local geometry where charges are evacuated through one electrode whereas spin diffusion can be collected by another nearby electrode [2, 3]. This lateral geometry is well suited to nanostructures, but it is limited by the required current densities and the short spin diffusion lengths [4]. Another option relies on using the spin Hall effect, a phenomenon based on the spin-orbit interaction of a charge current which generates a transverse spin current in a conductor [5, 6]. Pure spin currents can also be generated in ferromagnetic insulators by the spin pumping mechanism [7–9] during magnetization precession. This effect is produced by the damping of spin-waves which transfer angular momentum across an interface to a neighbouring layer. The emitted pure spin current can be detected electronically in an adjacent layer by the inverse spin Hall effect (ISHE) using metals with strong spin-orbit coupling like Pt [10, 11, 13, 14, 34]. The novelty here offered by electrical detection of the spin pumping using the ISHE is that it can be used also on non-metallic ferromagnets, including Yttrium Iron Garnet (YIG) [9, 15–20, 32, 33], a magnetic insulator which has unsurpassed small damping in ferromagnetic resonance (FMR). But so far, only the dc component of the ISHE voltage induced by FMR has been measured, which is a second order effect in the precession angle. Here, we report on a direct measurement of its first order ac counterpart.

The experiments of the present study are performed at room temperature on a YIG|Pt bi-layer where the YIG is a 200 nm thick epitaxial film grown by liquid phase epitaxy. A 6 nm thick Pt layer is then sputtered on top and two contact electrodes are defined at each end. The sample is mounted on a stripline antenna generating a microwave field h oscillating at a frequency f_p as sketched in Fig.1. At resonance of the uniform mode, the YIG emits, perpendicularly to the YIG|Pt interface, a flow of angular momentum generated by the spin pumping effect,

$$\boldsymbol{J}_s = \left(\frac{\hbar}{2eM_s}\right)^2 G_{\uparrow\downarrow}\left[\boldsymbol{M}\times\frac{\partial \boldsymbol{M}}{\partial t}\right] . \qquad (1)$$

In this expression, $\boldsymbol{M}$ is the magnetization vector, whose norm is M_s, $\hbar$ is the reduced Planck constant, e the electron charge, and $G_{\uparrow\downarrow}$ the spin mixing conductance at the YIG|Pt interface in units of $\Omega^{-1}{\cdot}\mathrm{m}^{-2}$. The spin current pumped into the adjacent Pt is then converted into a charge current by ISHE,

$$\boldsymbol{J}_c = \frac{2e}{\hbar}\Theta_{\mathrm{SH}}\left[\boldsymbol{y}\times\boldsymbol{J}_s\right] , \tag{2}$$

where Θ_{SH} is the spin Hall angle in Pt and $\boldsymbol{y}$ is the unit vector perpendicular to the interface (see Fig.1).

Importantly, the flow $\boldsymbol{J}_s$ (and hence $\boldsymbol{J}_c$) has both dc and ac components [23]. The dc part of this signal is normally detected as a voltage, proportional to $\boldsymbol{J}_c(\mathrm{dc})$, that is maximum in a transverse geometry (*i.e.* $\perp H$, see Fig.1a). In contrast, $\boldsymbol{J}_c(\mathrm{ac})$ is maximum in a parallel geometry (*i.e.* $\parallel H$, see Fig.1b). It is interesting to note that for circular precession the dc signal is second order in the precession angle θ ($\propto \sin^2\theta$, maximal for $\theta = 90°$), while its ac counterpart is first order ($\propto \sin\theta\cos\theta$ and maximal for $\theta = 45°$). Thus the ratio of ac to dc scales as $1/\tan\theta$, which is large for small precession angles. However, the ac component is much harder to detect as it oscillates obviously at the same frequency as that of the microwave generator producing the FMR. This microwave excitation field h induces eddy currents in any closed circuit containing the sample. These spurious ac currents are generally rather large and dominate any other contribution at the same frequency. Therefore, a clear detection of the ac spin currents has not yet been successful as one has to carefully eliminate the large amplitude eddy currents. In this letter, we report on the unambiguous detection of these ac spin currents emitted at ferromagnetic resonance using a specially designed system leading to an ac signal totally unpolluted by any other contribution. The key strategy here is to generate the FMR at half the frequency of the excitation source. This phenomenon is known as parametric excitation [24]. It exploits the fact that due to the ellipticity of the in-plane precession, the magnetization follows a clamshell trajectory. During a full revolution of $\boldsymbol{M}$ around its precession axis z, the z-component of the magnetization M_z oscillates twice faster, see Fig.1a. This is also illustrated in Fig.1b using red and blue colors to code its x-component, M_x. Therefore, by exciting parallel to $\boldsymbol{M}$, one can trigger the precession at half the source frequency. One should note however that this parallel parametric excitation is only possible in systems with low damping, since the excitation power needs to exceed a minimum threshold corresponding to a fraction of linewidth (typically below one Oersted for YIG [24]) in order to drive the magnetization into oscillation.

Experimentally, since the technique depends sensitively on the respective orientations of the microwave excitation and the bias field, we shall measure the ratio of the dc and ac components of $\boldsymbol{J}_c$, by rotating H, the static bias magnetic field, in the film plane. For all practical purposes, the YIG slab can be considered as an infinite film, whose resonance conditions are independent of the orientation of H.

In order to characterize our sample, and in particular the electrical conversion of the pumped spin current at the YIG|Pt interface, we first perform standard FMR resonance, where the small microwave field h is perpendicular to H ($\phi_H = 90°$). It is indeed the most efficient configuration to excite the magnetization dynamics: in the case displayed in Fig.2, the angle of precession induced in YIG at resonance by a microwave field $h = 36$ mOe ($P = -5$ dBm) is $\theta = 1.1°$ (see Supplementary Materials). The FMR signal is detected simultaneously by probing the power transmitted through the microwave line using a diode (Fig.2a) and by measuring the dc ISHE voltage transversally to the static magnetization (Fig.2b). Both measurements yield the same evolution of the resonance field versus frequency following the Kittel law for an in-plane magnetized thin film, see Fig.3a. By measuring the diode signal at low power ($P = -20$ dBm, corresponding to $h = 6$ mOe), one can also determine in the linear regime the dependence of the linewidth on frequency, which is reported in the inset of Fig.2a. A linear fit yields the Gilbert damping, $\alpha_G = (1.4 \pm 0.1) \cdot 10^{-4}$, highlighting the very small magnetic relaxation of our YIG film [33]. The inhomogeneous part to the linewidth, $\Delta H_0 = 1.7 \pm 0.2$ Oe, reflects sample imperfections specific to the growth process of this batch. We find that this contribution dominates the broadening below 10 GHz. The amplitude of $V_{\mathrm{ISHE}}(\mathrm{dc})$ measured at resonance allows us to determine the transport parameters at play in the electrical conversion of the pumped spin current (see Supplementary Materials). We find that our dc ISHE data can be well explained using typical parameters of the YIG|Pt system [32, 33]: spin diffusion length $\lambda_{\mathrm{sd}} = 2$ nm, spin Hall angle $\Theta_{\mathrm{SH}} = 0.05$, and spin mixing conductance $G_{\uparrow\downarrow} = 10^{14}\ \Omega^{-1} \cdot \mathrm{m}^{-2}$.

We now wish to excite parametrically the YIG magnetization at half the applied microwave frequency, $f_p/2$, by taking advantage of the clamshell shape of the precession trajectory, which is sketched in Fig.1. For this, the component of the microwave field h parallel to the bias field H should reach the excitation threshold for parallel parametric excitation [24]. To demonstrate this effect in our sample through dc ISHE voltage measurements, we set a finite angle $\phi_H = 10°$ between h and H (see inset of Fig.3b). Compared to the previous

perpendicular geometry, the resonance condition at f_p has not changed, only the microwave field is less efficient to bring the magnetization out-of-equilibrium, thus a stronger excitation power should be used to reach the same precession angle. We move momentarily to lower frequency in order to insert in the microwave circuit an additional amplifier limited in bandwidth to 1.1 GHz (see Supplementary Materials). At $f_p = 1.092$ GHz and $P = +19.8$ dBm we observe only one resonance peak at $H = 80$ Oe in Fig.3b. The new feature here is that if we increase the power to $P = +27.8$ dBm, a second peak appears in the spectrum at $H = 20$ Oe. Looking at the Kittel law of Fig.3a), we find that it corresponds to the uniform mode resonating at $f_p/2$, which is thus parametrically excited [17, 18, 25, 26]. Thanks to the quantitative analysis of $V_{\mathrm{ISHE}}(\mathrm{dc})$ using the transport parameters determined previously, it is possible to quantify the angle of precession corresponding to this parametric excitation: $\theta = 5.1°$ (see Supplementary Materials).

The next step is to directly detect the ac ISHE voltage generated at $f_p/2$ by the parametrically excited magnetization dynamics. For this, we now align the microwave field h with the bias field H ($\phi_H = 0°$) and excite the system at $f_p = 3.6$ GHz and high power, $P = +24$ dBm. The two voltage leads which contact the Pt layer are connected directly into a spectrum analyzer (SA) without any preamplification scheme. By sweeping the frequency of the SA at fixed $H = 205$ Oe, we detect a large signal of amplitude 30 μV at exactly $f_p/2 = 1.8$ GHz, as can be seen in Fig.4a. We claim this signal to be the ac component of the pure spin current pumped from the YIG parametric excitation into Pt, and converted into a voltage by ISHE. To prove this, we plot in Fig.4b the amplitude of the SA signal measured at $f_p/2$ as a function of H. We find that the amplitude of the signal is maximum at $H = 205$ G, which is the resonance field determined by standard FMR at 1.8 GHz in Fig.2, and dies out in a range of about ± 1.5 Oe around this field. We have also checked that this ac voltage signal has a parametric excitation origin, by studying its amplitude as a function of the excitation power. One can observe in the inset of Fig.4b that the peak at $f_p/2$ suddenly appears on the SA above a critical power $P_c = +20.7$ dBm, *i.e.*, a critical microwave field $h_c = 0.7$ Oe, in good agreement with the expected threshold for parallel parametric excitation in YIG [24]. We note that the envelope of the parametric excitation signal observed in Fig.4b as a function of H has a shape close to that of the standard FMR peak of Fig.2. Still, we observe abrupt jumps of the amplitude as H is varied. We find that the details of this variation are very sensitive to changes in the orientation ϕ_H of the bias

field. We attribute this to the excitation of spin-wave modes which are almost degenerate with the uniform precession mode [24, 27]. We have repeated the same experiment for different excitation frequencies ranging from 0.8 GHz up to 6 GHz. Because the microwave power exceeds the threshold for parallel parametric excitation ($P = +22$ dBm), an ac ISHE voltage at half the excitation frequency is observed on the SA as a function of H when the condition for resonance is met at $f_p/2$ (cf. Kittel law on Fig.5). Lastly, in order to check experimentally that our method eliminates *all* spurious signals, we performed the same series of measurements on a reference sample where the Pt layer was replaced by 15 nm of Al. We found experimentally that *no* electrical signal is produced at $f_p/2$, which allows to conclude that the layer with strong-spin orbit scattering like Pt is indispensable to observe the ac ISHE voltage.

To gain more insight into the ac ISHE voltage, we would like to comment on its amplitude. For that, we compare the ac and dc components using the $\phi_H = 10^\circ$ configuration (see Fig.3b). We measure an effective dc voltage $V_{\mathrm{ISHE}}(\mathrm{dc}) = 1.1\ \mu\mathrm{V}$, while in the same conditions, the generated ac voltage is $V_{\mathrm{ISHE}}(\mathrm{ac}) = 6.2\ \mu\mathrm{V}$ (see Supplementary Materials). Thus, we obtain the experimental ratio $\left[V_{\mathrm{ISHE}}(\mathrm{ac})/V_{\mathrm{ISHE}}(\mathrm{dc})\right]_{\mathrm{exp}} = 5.6$. We have determined that the angle of precession corresponding to the parametric excitation observed at $H = 20$ Oe is $\theta = 5.1^\circ$. Therefore, one would expect that $\left[J_s(\mathrm{ac})/J_s(\mathrm{dc})\right]_{\mathrm{theo}} = \xi/\tan\theta = 5.7$, where $\xi = 0.51$ is the ellipticity correction factor for this case (see Supplementary Materials), in excellent agreement with our estimation above.

In conclusion, we have shown that the microwave part of the spin pumping current emitted by a ferromagnet driven at resonance can be detected by the inverse spin Hall effect using an adjacent metallic layer with strong spin-orbit scattering [28]. On our millimeter size YIG|Pt sample it leads to a micro-Volt range microwave signal measurable directly on a spectrum analyzer without any pre-amplification or impedance matching. We believe that this broad band direct detection provides a novel efficient means to study magnetization dynamics in a wide variety of ferromagnetic materials. Further analysis of the measured spectra in the parallel parametric geometry will provide new insights into the spin-wave competition in the nonlinear regime. The phenomenon will also allow dynamical studies of the process of spin transfer at the interface with strong spin orbit non-magnetic metals [29–31].

This research was supported by the French ANR Grant Trinidad (ASTRID 2012 program) and by the RTRA-2011 grant Spinoscopy.

Supplementary Materials: Sample preparation and characterization

The 200 nm thick single crystal $Y_3Fe_5O_{12}$ (YIG) film was grown by liquid phase epitaxy on a (111) $Gd_3Ga_5O_{12}$ (GGG) substrate. A 6 nm thin Pt layer with conductivity $\sigma = (2.3 \pm 0.2) \cdot 10^6\ \Omega^{-1} \cdot m^{-1}$ was then sputtered on top. Vibrating sample magnetometry reveals that the YIG film does not exhibit any in-plane anisotropy and has both very low coercivity (0.5 Oe) and saturation field (2 Oe). Its saturation magnetization, $M_s = 139$ emu·cm^{-3}, is the one of bulk YIG. This value was confirmed by in-plane broadband FMR (from 0.4 GHz up to 17 GHz). FMR also allows to extract the gyromagnetic ratio, $\gamma = 1.785 \cdot 10^7$ rad·s^{-1}·Oe^{-1}.

Experimental setup

Experiments are performed at room temperature. The microwave cell is placed at the center of an electromagnet which can be rotated. The 500 μm wide, 2 μm thick Au transmission line cell is connected to a synthesizer providing frequencies up to 20 GHz and power up to +24 dBm (additional boost to +35 dBm is obtained by using an external amplifier for frequencies lower than 1.1 GHz). A standard diode provides a quadratic detection of the transmitted power. The calibration of the linearly polarized in-plane microwave field yields $h = 60$ mOe when the output power is 0 dBm. The YIG|Pt sample is cut into a slab with lateral dimensions of 1.7 mm $\times$ 7 mm and placed on top of the transmission line. The sample is mounted upside-down on the stripline with the Pt layer facing the Au antenna. The two voltage leads are equidistant from the area of excitation and separated by 3 mm (the two-point resistance is $R = 129\ \Omega$). $V_{\mathrm{ISHE}}(\mathrm{dc})$ is measured by a lock-in technique with the microwave power turned on and off at a frequency of 1.9 kHz. $V_{\mathrm{ISHE}}(\mathrm{ac})$ is directly measured using a spectrum analyzer (input impedance $Z_0 = 50\ \Omega$). Due to impedance mismatch, the voltage transmission coefficient from the YIG|Pt sample to the spectrum analyzer is $T = 1 - \frac{R - Z_0}{R + Z_0} = 0.56$. We have checked that this value holds below 2 GHz using a network analyzer.

Analysis of the dc ISHE voltage

The amplitude of the ISHE dc voltage generated in Pt by the magnetization precession with an angle θ at frequency f in YIG is given by [32, 33]:

$$V_{\rm ISHE}({\rm dc}) = \Theta_{\rm SH} \frac{G_{\uparrow\downarrow}}{G_{\uparrow\downarrow} + \frac{\sigma}{\lambda_{\rm sd}} \frac{1-\exp\left(-2t/\lambda_{\rm sd}\right)}{1+\exp\left(-2t/\lambda_{\rm sd}\right)}} \sin(\phi_H) \frac{\pi\hbar L \mathcal{E} f \sin^2(\theta)}{et} \frac{\left(1-\exp\left(-t/\lambda_{\rm sd}\right)\right)^2}{1+\exp\left(-2t/\lambda_{\rm sd}\right)} \ . \quad (3)$$

In this expression, $G_{\uparrow\downarrow}$ is the spin mixing conductance, σ the conductivity of the Pt layer, $\Theta_{\rm SH}$ its spin Hall angle, $\lambda_{\rm sd}$ its spin diffusion length, t its thickness, and L the length of the sample excited by the excitation field. $\mathcal{E}$ is a factor close to unity, which depends on the ellipticity of the precession trajectory, hence on the frequency $\omega/2\pi$ [34]: in our case, $\mathcal{E} = 0.43$ at 0.546 GHz and $\mathcal{E} = 1.06$ at 1.8 GHz.

The dc ISHE voltage is maximal when the angle ϕ_H between the direction along which the voltage drop is measured and the static magnetization equals 90°, which is the case in our standard FMR geometry (Fig.2). In this case, we have checked that the dc ISHE voltage is odd in applied magnetic field, which shows that the voltage generated at resonance is not due to a thermoelectrical effect. The measured $V_{\rm ISHE}({\rm dc})$ are in good agreement with Eq.(3), using values estimated from high frequency susceptibility for the precession angle θ and the following typical transport parameters [33]: $\Theta_{\rm SH} = 0.05$; $\lambda_{\rm sd} = 2$ nm; $G_{\uparrow\downarrow} = 10^{14}\ \Omega^{-1}{\cdot}{\rm m}^{-2}$. For instance, at $f_p = 1.8$ GHz and $P = -5$ dBm, the angle of precession at resonance is estimated to be $\theta = 1.1°$, which yields $V_{\rm ISHE}({\rm dc}) = 0.44\ \mu$V, to be compared to the value of 0.5 μV measured in Fig.2b. The overall agreement between Eq.(3) and the experimental measurements of $V_{\rm ISHE}({\rm dc})$ vs. power (from -20 dBm to +10 dBm) and frequency (from 0.4 to 17 GHz) is within 30%.

When the angle $\phi_H = 10°$, as in the parametric excitation geometry of Fig.3b, the loss of sensitivity for the dc ISHE voltage drops as $1/\sin\phi_H \simeq 5.7$. Experimentally, we measure that at $P = +27.8$ dBm, the parametric excitation at $f_p/2 = 0.546$ GHz generates a dc voltage $V_{\rm ISHE}({\rm dc}) = 0.19\ \mu$V (setting $\phi_H = -10°$ leads to a measured dc ISHE voltage of same amplitude but opposite sign). Using the same parameters as for the analysis in the standard FMR configuration, we can estimate the corresponding angle of precession from Eq.(3): $\theta = 5.1°$.

Analysis of the ac ISHE voltage

In order to calculate the ac spin current generated by an elliptical precession trajectory, we follow the analysis performed to derive the factor $\mathcal{E}$ in Eq.(3) for the dc ISHE voltage [34]. To do so, we use the Landau-Lifschitz-Gilbert equation to compute at resonance the three components of the magnetization precessing around its equilibrium axis z and the expression of the pumped spin current flowing accross the FM|NM interface (see Eq.(1) of main text).

In the case of a circular precession, this yields $J_{s,x}^{\rm circ}(t) = -\omega \left(\frac{\hbar}{2e}\right)^2 G_{\uparrow\downarrow} \sin\theta\cos\theta\sin\omega t$ and $J_{s,z}^{\rm circ} = \omega \left(\frac{\hbar}{2e}\right)^2 G_{\uparrow\downarrow} \sin^2\theta$. (In our geometry, $J_{s,y}^{\rm circ}(t)$ does not produce any charge current through ISHE because its spin polarization is parallel to the normal y of the FM|NM interface, see Eq.(2) and Fig.1 of main text). Hence, $|J_s^{\rm circ}({\rm ac})|/J_s^{\rm circ}({\rm dc}) = 1/\tan\theta$, where θ is the angle of precession.

In the case of an elliptical precession, the same approach yields the correction factors with respect to the circular case:

- $J_s({\rm dc})/J_s^{\rm circ}({\rm dc}) = \frac{2\omega(\omega_M+\sqrt{\omega_M^2+4\omega^2})}{\omega_M^2+4\omega^2}$, for the dc component of the pumped spin current. This is nothing else than the factor $\mathcal{E}$ appearing in Eq.(3) [34].

- $J_s({\rm ac})/J_s^{\rm circ}({\rm ac}) = \frac{2\omega}{\sqrt{\omega_M^2+4\omega^2}}$ for its ac component.

In these expressions, $\omega_M = \gamma 4\pi M_s$. Hence, the ratio of the ac and dc components writes:

$$\frac{J_s({\rm ac})}{J_s({\rm dc})} = \frac{\sqrt{\omega_M^2+4\omega^2}}{\omega_M+\sqrt{\omega_M^2+4\omega^2}}\frac{1}{\tan\theta} = \frac{\xi}{\tan\theta}\,. \tag{4}$$

Using the same transport parameters as for the analysis of the dc ISHE voltage, one finds that the precession angle corresponding to the 30 μV ac ISHE voltage measured in Fig.4 at $f_p/2 = 1.8$ GHz equals $\theta = 2.5°$. In this experiment, $\phi_H = 0°$, so that the corresponding dc voltage vanishes (see Eq.(3)).

Setting $\phi_H = 10°$, as in the experiment of Fig.3b, enables to detect both the dc and ac voltages. As explained above, the angle of precession estimated from the dc ISHE voltage at $f_p/2 = 0.546$ GHz is $\theta = 5.1°$. It corresponds to an effective dc voltage $V_{\rm ISHE}({\rm dc}) = 1/\sin\phi_H \times 0.19$ μV$= 1.1$ μV. The ac ISHE voltage measured in the same conditions is found to be 3.5 μV. This value has to be corrected due to the previously mentioned impedance mismatch, $V_{\rm ISHE}({\rm ac}) = 1/T \times 3.5$ μV$= 6.2$ μV. Hence, the experimental ratio between the

ac and dc components of the ISHE voltage current is $[V_{\rm ISHE}({\rm ac})/V_{\rm ISHE}({\rm dc})]_{\rm exp} = 5.6$, which is in very good agreement with the theoretical value from Eq.(4), $[J_s({\rm ac})/J_s({\rm dc})]_{\rm theo} = 5.7$.

---

* Corresponding author: oklein@cea.fr

[1] T. Jungwirth, J. Wunderlich, and K. Olejnik, Nature Materials **11**, 382 (2012)

[2] S. O. Valenzuela and M. Tinkham, Nature (London) **442**, 176 (2006)

[3] T. Kimura, Y. Otani, T. Sato, S. Takahashi, and S. Maekawa, Phys. Rev. Lett. **98**, 156601 (2007)

[4] Y. Otani and T. Kimura, IEEE Trans. Magn. **44**, 1911 (20008)

[5] M. I. Dyakonov and V. I. Perel, JETP Lett. **13**, 467 (1971)

[6] J. E. Hirsch, Phys. Rev. Lett. **83**, 1834 (1999)

[7] Y. Tserkovnyak, A. Brataas, G. E. W. Bauer, and B. I. Halperin, Rev. Mod. Phys. **77**, 1375 (2005)

[8] G. Woltersdorf, M. Buess, B. Heinrich, and C. H. Back, Phys. Rev. Lett. **95**, 037401 (2005)

[9] B. Heinrich, C. Burrowes, E. Montoya, B. Kardasz, E. Girt, Y.-Y. Song, Y. Sun, and M. Wu, Phys. Rev. Lett. **107**, 066604 (2011)

[10] E. Saitoh, M. Ueda, H. Miyajima, and G. Tatara, Appl. Phys. Lett. **88**, 182509 (2006)

[11] K. Ando, Y. Kajiwara, S. Takahashi, S. Maekawa, K. Takemoto, M. Takatsu, and E. Saitoh, Phys. Rev. B **78**, 014413 (2008)

[12] K. Ando, T. Yoshino, and E. Saitoh, Appl. Phys. Lett. **94**, 152509 (2009)

[13] O. Mosendz, J. E. Pearson, F. Y. Fradin, G. E. W. Bauer, S. D. Bader, and A. Hoffmann, Phys. Rev. Lett. **104**, 046601 (2010)

[14] O. Mosendz, V. Vlaminck, J. E. Pearson, F. Y. Fradin, G. E. W. Bauer, S. D. Bader, and A. Hoffmann, Phys. Rev. B **82**, 214403 (2010)

[15] Y. Kajiwara, K. Harii, S. Takahashi, J. Ohe, K. Uchida, M. Mizuguchi, H. Umezawa, H. Kawai, K. Ando, K. Takanashi, S. Maekawa, and E. Saitoh, Nature (London) **464**, 262 (2010)

[16] Z. Wang, Y. Sun, M. Wu, V. Tiberkevich, and A. Slavin, Phys. Rev. Lett. **107**, 146602 (2011)

[17] C. W. Sandweg, Y. Kajiwara, A. V. Chumak, A. A. Serga, V. I. Vasyuchka, M. B. Jungfleisch, E. Saitoh, and B. Hillebrands, Phys. Rev. Lett. **106**, 216601 (2011)

[18] H. Kurebayashi, O. Dzyapko, V. E. Demidov, D. Fang, A. J. Ferguson, and S. O. Demokritov,

Nature Mater. (London) **10**, 660 (2011)

[19] L. H. Vilela-Leão, C. Salvador, A. Azevedo, and S. M. Rezende, Appl. Phys. Lett. **99**, 102505 (2011)

[20] A. V. Chumak, A. A. Serga, M. B. Jungfleisch, R. Neb, D. A. Bozhko, V. S. Tiberkevich, and B. Hillebrands, Appl. Phys. Lett. **100**, 082405 (2012)

[21] V. Castel, N. Vlietstra, J. Ben Youssef, and B. J. van Wees, Appl. Phys. Lett. **101**, 132414 (2012)

[22] C. Hahn, G. de Loubens, O. Klein, M. Viret, V. V. Naletov, and J. Ben Youssef, Phys. Rev. B **87**, 174417 (2013)

[23] H. Jiao and G. E. W. Bauer, Phys. Rev. Lett. **110**, 217602 (2013)

[24] M. Sparks, *Ferromagnetic relaxation theory* (McGraw-Hill, New York, 1964)

[25] H. Kurebayashi, O. Dzyapko, V. E. Demidov, D. Fang, A. J. Ferguson, and S. O. Demokritov, Appl. Phys. Lett. **99**, 162502 (2011)

[26] K. Ando and E. Saitoh, Phys. Rev. Lett. **109**, 026602 (2012)

[27] V. V. Naletov, G. de Loubens, V. Charbois, O. Klein, V. S. Tiberkevich, and A. N. Slavin, Physical Review B **75**, 140405 (Apr. 2007)

[28] During this work, we became aware of a parallel effort reporting also detection of ac-ISHE but in NiFe|Pt: http://arxiv.org/abs/1307.2961

[29] X. Jia, K. Liu, K. Xia, and G. E. W. Bauer, Europhys. Lett. **96**, 17005 (2011)

[30] L. Liu, C.-F. Pai, Y. Li, H. W. Tseng, D. C. Ralph, and R. A. Buhrman, Science **336**, 555 (2012)

[31] I. M. Miron, K. Garello, G. Gaudin, P.-J. Zermatten, M. V. Costache, S. Auffret, S. Bandiera, B. Rodmacq, A. Schuhl, and P. Gambardella, Nature **476**, 189 (2011)

[32] V. Castel, N. Vlietstra, J. Ben Youssef, and B. J. van Wees, Appl. Phys. Lett. **101**, 132414 (2012).

[33] C. Hahn, G. de Loubens, O. Klein, M. Viret, V. V. Naletov, and J. Ben Youssef, Phys. Rev. B **87**, 174417 (2013).

[34] K. Ando, T. Yoshino, and E. Saitoh, Appl. Phys. Lett. **94**, 152509 (2009).

FIGURES

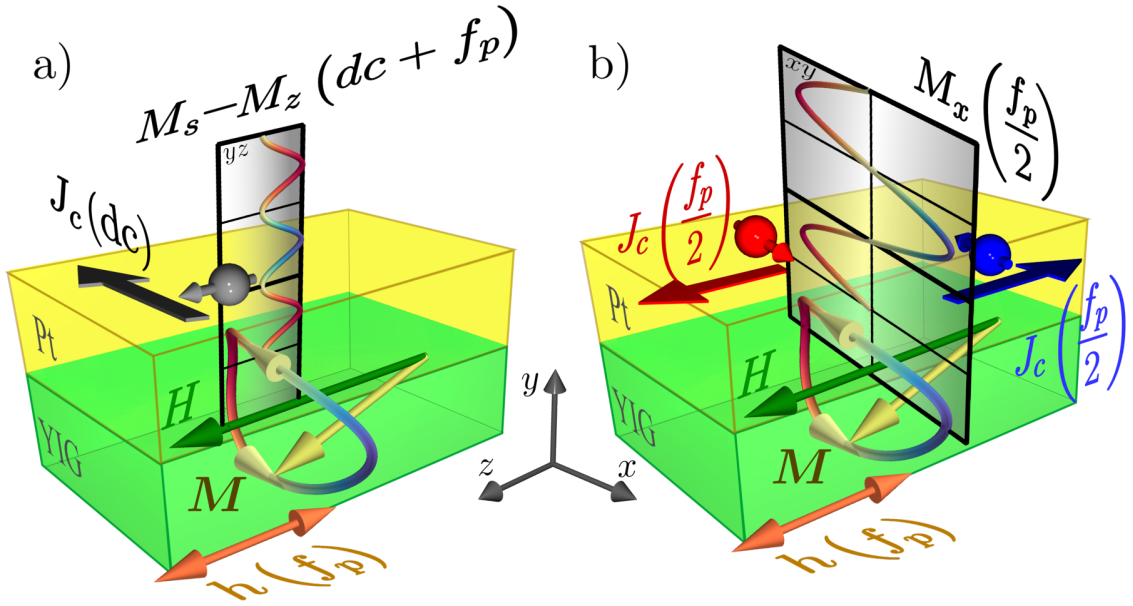

FIG. 1. (Color online) Schematic representation showing the direction of the dc (a) and ac (b) charge currents produced when a pure spin current is pumped from the insulating magnetic YIG (green) into the strong spin-orbit Pt metal (yellow). The instantaneous magnetization $\boldsymbol{M}(t)$ is shown in a bi-variate colormap: the blue-red colors code the x-component and the gray shades code the z-component. The precession of $\boldsymbol{M}$ at $f_p/2$ around $\boldsymbol{z}$, is driven by parametric excitation: it requires the pumping field h, oscillating at f_p, to be parallel to the bias magnetic field H, and the precession of (M_x, M_y) to be elliptic (thus $M_x^2 + M_y^2$ is not a constant of the motion). The flowcharts on top illustrate that $M_z = \sqrt{M_s^2 - M_x^2 - M_y^2}$ then oscillates twice faster than M_x or M_y. Spin pumping currents are flowing from YIG to Pt (*i.e.* along the y-axis). The injected angular momentum in Pt is carried by the spins (arrows attached to the electrons opposite to their angular momentum). The direction of the instantaneous charge current (flat arrow) is given by the right hand rule, see Eq.(2).

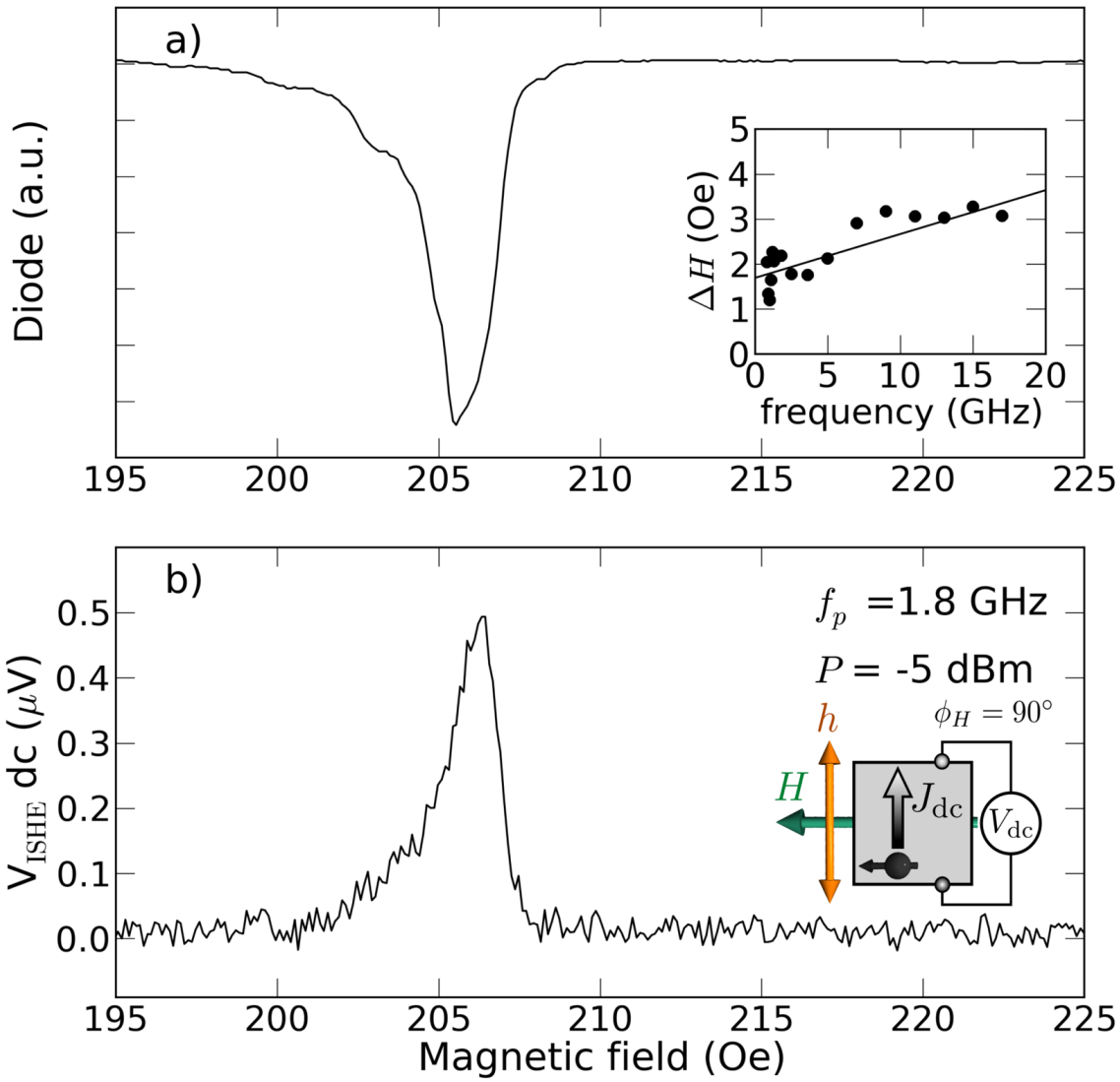

FIG. 2. (Color online) Standard FMR detected using dc ISHE voltage. The pumping field h oscillating at $f_p = 1.8$ GHz is oriented perpendicularly to the static magnetic field H. (a) Larmor absorption peak of the uniform mode detected with a diode (the inset shows the dependence of the linewidth on frequency). (b) Corresponding dc ISHE voltage measured perpendicularly to H (the inset shows the geometry of the experiment).

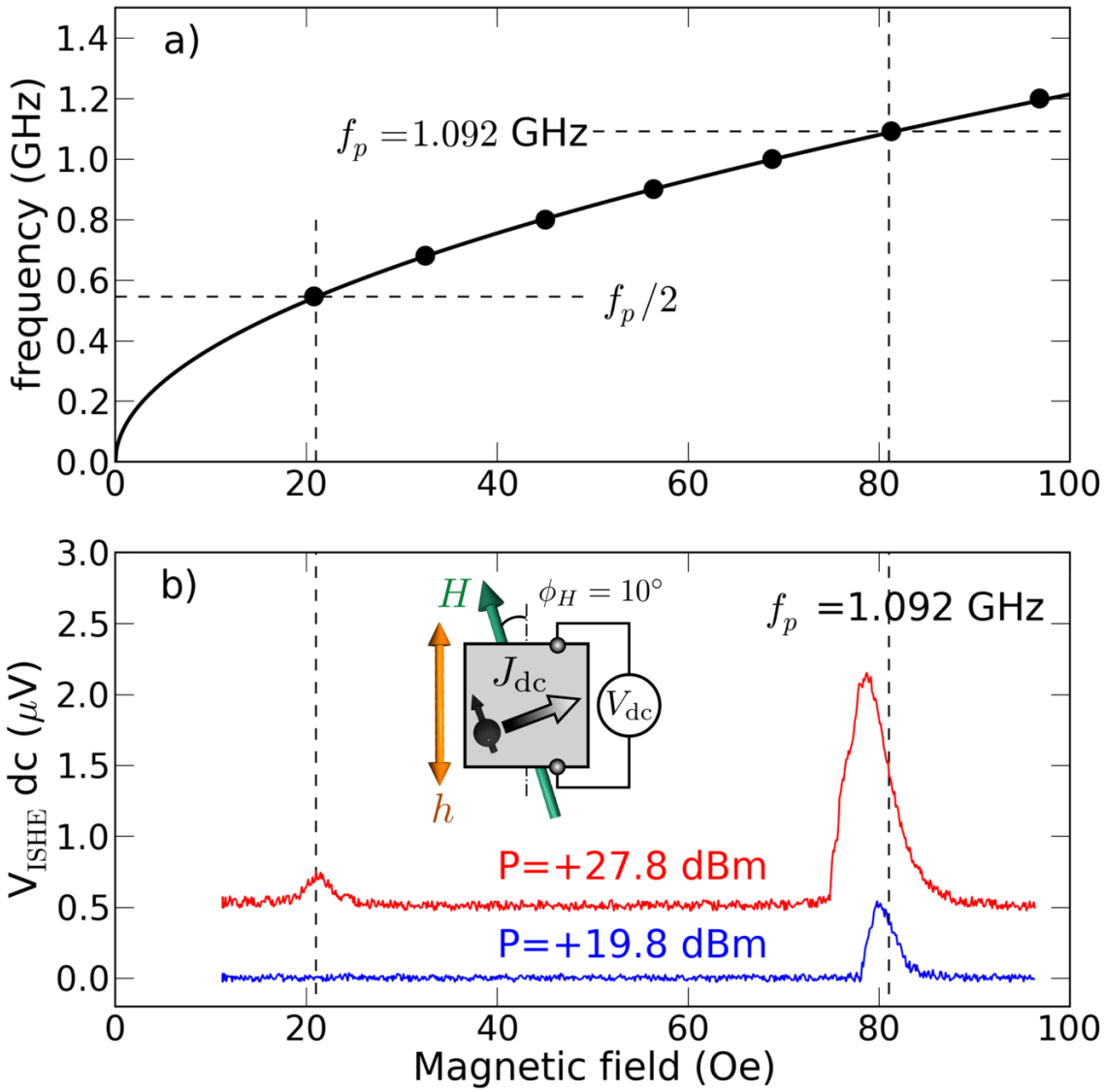

FIG. 3. (Color online) Parametric excitation detected using the dc ISHE voltage. (a) Measured variation of the resonance frequency $f_{\rm res}$ as a function of the applied field (dots) using the standard FMR geometry (Fig.2). The solid line is the Kittel law $f_{\rm res} = (\gamma/2\pi)\sqrt{H(H+4\pi M_s)}$ with $\gamma = 1.785 \cdot 10^7$ rad·s^{-1}·Oe^{-1} and $M_s = 139$ emu·cm^{-3}. (b) Spin wave mode spectra detected using the dc ISHE voltage for two different power levels. The bias field H is oriented at 10° from the pumping field h oscillating at $f_p = 1.092$ GHz (the inset shows the geometry of the experiment). At lower power (+19.8 dBm), the only peak detected in the spectrum occurs when the Larmor condition is met at f_p. At higher power (+27.8 dBm), a new peak appears in the spectrum at $f_p/2$, corresponding to the parametrically excited resonance.

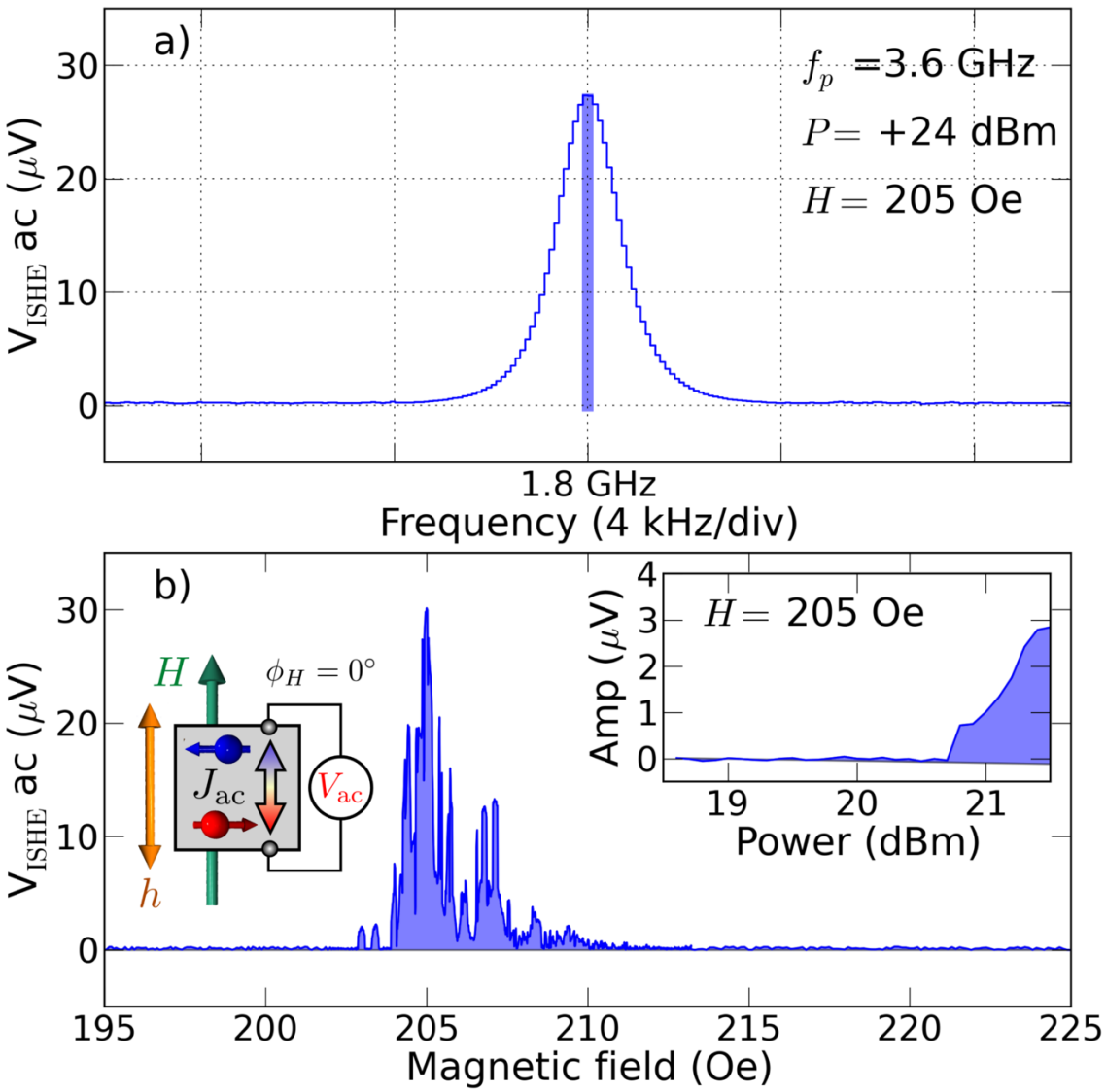

FIG. 4. (Color online) Parametric excitation detected using the ac ISHE voltage. The large power (+24 dBm) pumping field h at $f_p = 3.6$ GHz is oriented parallel to the static magnetic field H. (a) The ac ISHE voltage generated by the parametric excitation at $H = 205$ Oe is monitored on a spectrum analyzer (1 kHz resolution bandwidth): an oscillation voltage is detected at $f_p/2 = 1.8$ GHz. (b) The amplitude of this oscillation is measured as the bias field is swept from 195 to 225 Oe. The envelope of the curve should be compared to that in Fig.2. The maximum parametric signal occurs at $H_{\rm res} = 205$ Oe. The inset shows the threshold behavior ($P_c \simeq +20.7$ dBm) of the power dependence of the spectrum analyzer signal at 1.8 GHz to demonstrate the parametric excitation.

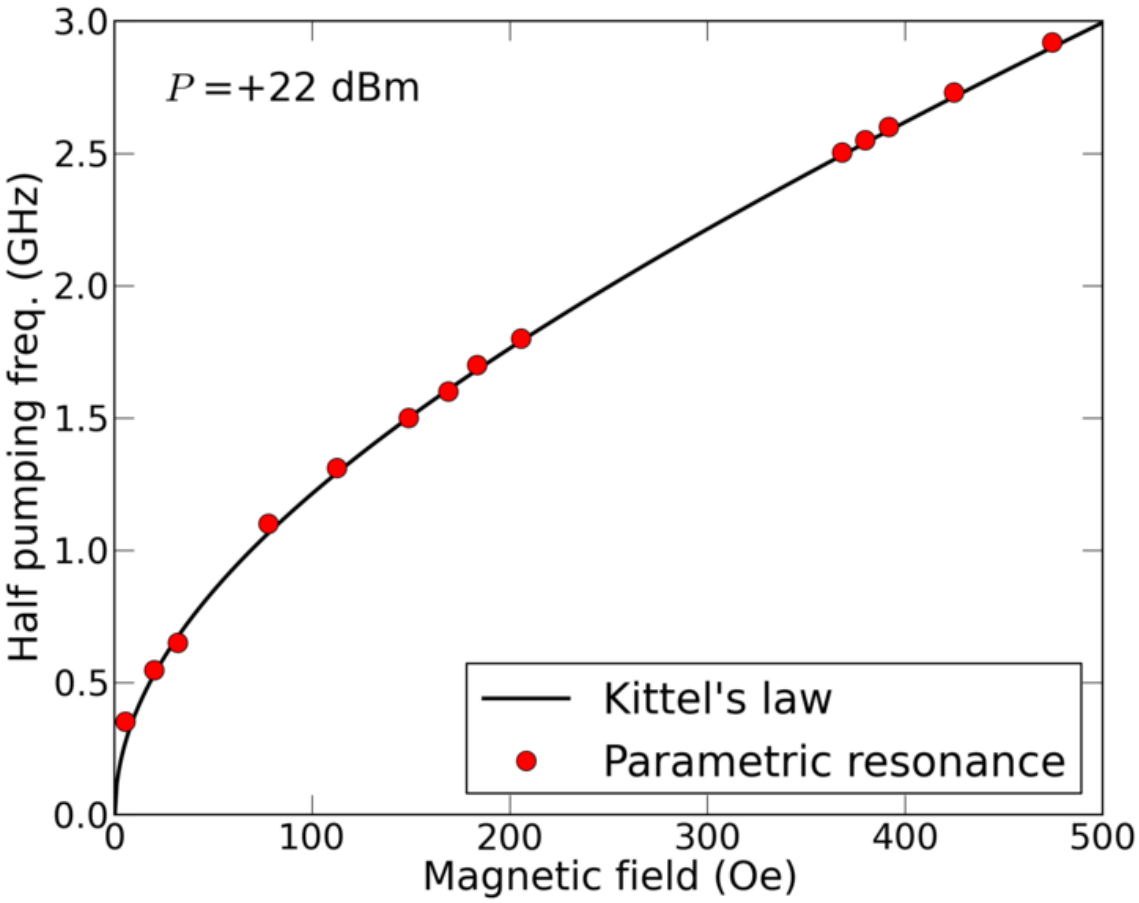

FIG. 5. (Color online) voltage at half the pumping frequency. Red dots correspond to the bias field required to observe the maximum parametric signal detected on the spectrum analyzer at $f_p/2$. The solid line is the Kittel law of the YIG|Pt bilayer (see Fig.3a).